Chemical Science

EDGE ARTICLE

View Article Online
View Journal | View Issue

Cite this: *Chem. Sci.*, 2015, **6**, 7258

Discovery of low energy pathways to metal-mediated B═N bond reduction guided by computation and experiment†

Tyler J. Carter,[a] Zachariah M. Heiden*[b] and Nathaniel K. Szymczak*[a]

Received 29th June 2015
Accepted 24th September 2015

DOI: 10.1039/c5sc02348c

www.rsc.org/chemicalscience

This manuscript describes a combination of DFT calculations and experiments to assess the reduction of borazines (B–N heterocycles) by η^6-coordination to $Cr(CO)_3$ or $[Mn(CO)_3]^+$ fragments. The energy requirements for borazine reduction are established as well as the extent to which coordination of borazine to a transition metal influences hydride affinity, basicity, and subsequent reduction steps at the coordinated borazine molecule. Borazine binding to $M(CO)_3$ fragments decreases the thermodynamic hydricity by >30 kcal mol^{-1}, allowing it to easily accept a hydride. These hydricity criteria were used to guide the selection of appropriate reagents for borazine dearomatization. Reduction was achieved with an H_2-derived hydride source, and importantly, a pathway which proceeds through a single electron reduction and H-atom transfer reaction, mediated by anthraquinone was uncovered. The latter transformation was also carried out electrochemically, at relatively positive potentials by comparison to all prior reports, thus establishing an important proof of concept for any future electrochemical B═N bond reduction.

1. Introduction

Due to a recognition of the finite availability of fossil fuels, considerable effort has been devoted to the development of new methods that generate, store, and use alternative energy vectors.[1,2] Hydrogen is a particularly promising energy carrier; however, several key challenges must be overcome prior to implementation.[3,4] In particular, reversible high-capacity hydrogen storage materials are required.[5] Ammonia borane (AB; NH_3BH_3) and related C–B–N compounds show great promise due to their high gravimetric and volumetric hydrogen capacities as well as the relative ease with which they can be dehydrogenated.[6–10] Dehydrogenation pathways of B–N compounds can vary depending on reaction conditions; however, thermal and catalytic dehydrogenation often affords cyclic oligomers, such as borazines and polyborazylene (PB), as spent fuel products.[10–13]

Borazines (and other related B–N heterocycles) have been a topic of interest to inorganic chemists for decades.[14,15] Early studies with this class of compounds probed electronic and reactivity parallels with arenes, since they are isostructural and isoelectronic with borazines.[14–17] However, despite these similarities, borazines exhibit marked differences in their electronic structure and reactivity. Recently, borazines have been identified as a terminal dehydrogenation product from spent B–N hydrogen storage materials, and in this context, borazines pose a unique challenge to reversible H_2 storage due to the thermodynamically strong B–N bonds.[16–20] The highly exergonic nature of the dehydrogenation reaction of B–N compounds has made the development of low-energy methods (Scheme 1) for the net-hydrogenation of borazine, and PB, a topic of great interest to the hydrogen storage community. While a few notable examples of borazine/PB recycling to AB exist,[21–26] all of these methods rely on energetically costly reagents which limit the net energy balance of the hydrogen storage system. Thus, a lower energy route to achieve reductive transformations of borazines would be beneficial. One strategy to lower the energetic barrier associated with reductive transformations of B–N heterocycles is through the coordination of borazine to a transition metal.[27,28]

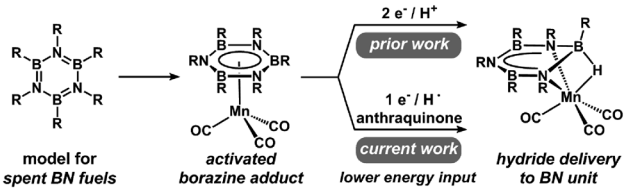

Scheme 1 Reaction pathways for hydride delivery to a Mn–borazine complex.

[a]*Department of Chemistry, University of Michigan, 930 N. University, Ann Arbor, MI 48109, USA. E-mail: nszym@umich.edu*

[b]*Department of Chemistry, Washington State University, PO Box 644630, Pullman, WA 99164, USA. E-mail: zachariah.heiden@wsu.edu*

† Electronic supplementary information (ESI) available: Spectral and electrochemical data and computational details. See DOI: 10.1039/c5sc02348c

Recent work in our group demonstrated that η^6-coordination of borazines to $Cr(CO)_3$ or $[Mn(CO)_3]^+$ fragments facilitates the addition of H^- or CH_3^- nucleophiles to afford dearomatized borazine complexes.[27,28] Metal-mediated reduction of borazines was also achieved *via* successive delivery of two-electrons and an exogenous proton donor, which represents an important step toward a potential (electro)catalytic regeneration scheme. In order to further interrogate one- and two-electron pathways for B=N bond reduction and to assess energetic costs, we sought to evaluate the thermodynamic requirements, as well as possible mechanistic pathways for these reactions. However, there are currently no data available that describe how the coordination of borazine to a transition metal fragment impacts reductive reactions.

In this study, we quantitatively describe the extent to which metal-mediated binding promotes the ionic hydrogenation of B=N bonds. We assess these values by the direct comparison of pK_a values and thermodynamic hydricities (ΔG_{H^-}) before and after coordination of the borazine to a transition-metal fragment. Additionally, the free energy values for the net-hydrogenation reactions have been used to guide the selection of mild reducing agents capable of promoting reduction. These insights provide direction for the targeted discovery of new pathways for the reduction of heterocyclic B–N bonds, which are relevant for the regeneration of spent AB fuels as well as other C–B–N heterocycles.[6–8,25,29,30]

2. Results and discussion

2.1. Free energy of hydrogen addition to $H_3B_3N_3H_3$ and $Me_3B_3N_3Me_3$

Alkyl substituted borazines have been used as model complexes to study the reactivity of borazine (and B–N spent fuels) due to their ease of synthesis, thermal stability, and low volatility. Despite these similarities, no direct comparison of the structural and thermodynamic properties of these two compounds has been reported. The parent borazine ($H_3B_3N_3H_3$) is volatile and readily cross links upon heating;[12] properties which have prevented the isolation of $H_3B_3N_3H_3$ transition metal complexes. In contrast, substituted borazines are less volatile and thermally robust, thus, our initial studies focused on $Cr(CO)_3$ (**1**) and $[Mn(CO)_3]^+$ (**2**) complexes of $Me_3B_3N_3Me_3$, which are readily isolable. We hypothesize that coordination of the B–N heterocycle to a transition metal can greatly influence its reduction chemistry. To evaluate this effect for $M(CO)_3$ units, we computationally assessed differences in the thermodynamics of H_2 addition reactions to borazines.

Previous computational studies have explored the thermodynamics of B–N spent fuel hydrogenation[18–20,31,32] and the nature of the M–borazine bond in theoretical $H_3B_3N_3H_3$ complexes.[33,34] To our knowledge, a direct comparison of the free energy of H_2 addition to the parent borazine *vs.* its alkyl substituted derivatives, as well as the extent of borazine activation and the effect on subsequent reduction following coordination, remains unexplored. To benchmark our computational model, the free energy of H_2 addition was calculated for the parent and alkylated borazines using the B3LYP or M06-2X functionals with the 6-31G(d,p) basis set in the gas phase for geometry optimizations. More accurate energies were obtained through a single point energy calculation using the 6-311++G(d,p) basis set in Et_2O (solvent selected for its compatibility with M–borazine complexes) using the polarized continuum solvation model.[35,36]

The B3LYP functional provided vibrational frequencies and redox potentials closest to the experimental values of the borazine metal complexes, *vida infra*, and was implemented in all subsequent computational analysis. The predicted free energy (Scheme 2, top) for the reduction of borazine ($H_3B_3N_3H_3$) to cyclotriborazane ($H_6B_3N_3H_6$) was compared with other computational studies and our calculated values slightly overestimate the free energy of borazine hydrogenation (53.5 kcal mol^{-1} for B3LYP and 45.0 for M06-2X in the gas phase) compared with the values predicted by Matus *et al.* (43.3 kcal mol^{-1}) and Miranda and Ceder (approximately 48 kcal mol^{-1}).[19,20] The slight overestimation in the free energy for the reduction of borazine using the B3LYP functional is attributed to the limited ability of the B3LYP functional to describe dative interactions.[19,37] However, our calculated enthalpy of H_2 addition of 1.4 kcal mol^{-1} is in good agreement with the experimental value of 1 kcal mol^{-1} reported by Schellenberg and Wolf.[38] Finally, we performed a NICS(0) calculation to evaluate aromaticity, and found a similar aromatic character between borazine and hexamethylborazine (see ESI†).[39–42] This result further validates that hexamethylborazine is a suitable model for borazine.[43]

The only known transition metal complexes of borazines are those of alkyl substituted variants.[27,28,44–49] Thus, determination of the thermodynamics of H_2 addition for both the parent and alkylated borazines is essential to establish general relationships of alkyl borazine coordinated metal complexes,[27,28] as model substrates for metal-mediated borazine reductions. In support, the addition of a single equivalent of H_2 to form a 1,2-H_2-borazine was predicted to have a nearly identical reaction free energy ($\Delta G = 31.9$ *vs.* 28.8 kcal mol^{-1}) for both the parent and alkylated borazines in Et_2O solutions (Scheme 2).

Although the first B=N bond reduction was found to be similar in energy for $H_3B_3N_3H_3$ and $Me_3B_3N_3Me_3$, the free energy for further reductions differed for each compound. For instance, while the reduction of $H_4B_3N_3H_4$ to cyclotriborazane ($H_6B_3N_3H_6$) is essentially thermo-neutral ($\Delta G = -1$ kcal mol^{-1}), the analogous H_2 addition steps for $Me_3HB_3N_3HMe_3$ are substantially higher in energy ($\Delta G = 30$ kcal mol^{-1}). Given the

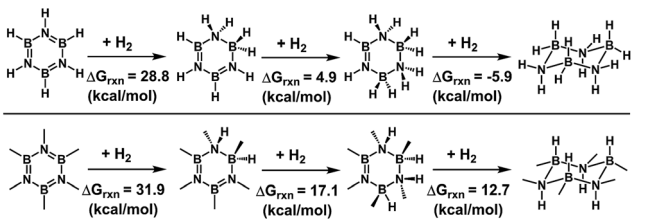

Scheme 2 Calculated free energy of hydrogenation for $H_3B_3N_3H_3$ and $Me_3B_3N_3Me_3$ in Et_2O solutions using the B3LYP/6-311G++(d,p)//B3LYP/6-31G(d,p) level of theory.

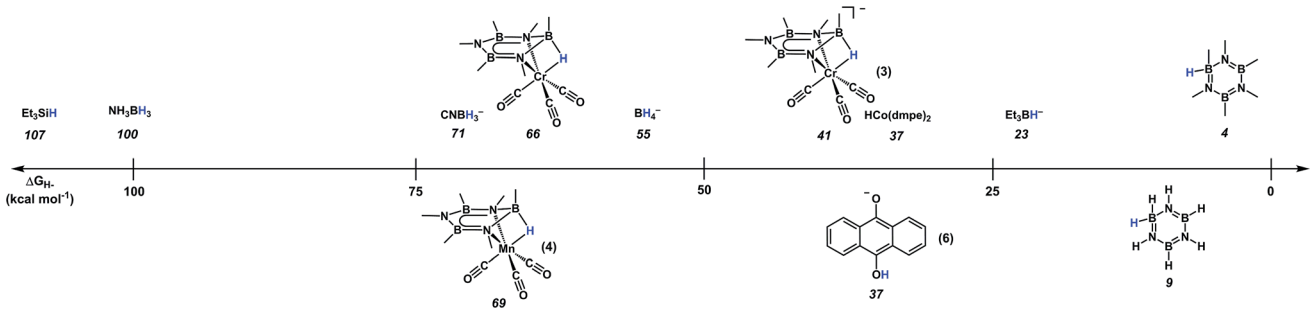

Scheme 3 Computational thermodynamic hydricity values (ΔG_{H^-}) for borazines, M–borazine complexes, and several common hydride sources in Et_2O solutions.

similarity of free energies for the first addition of H_2 to the borazine ring between $H_3B_3N_3H_3$ and $Me_3B_3N_3Me_3$, these data clearly demonstrate that $Me_3B_3N_3Me_3$ is a suitable model for mechanistic studies aimed at uncovering a route to reduce the thermodynamically most challenging B=N bonds *via* metal-mediated ionic hydrogenations.

In addition to the reduction of free borazines, we evaluated the extent to which $Me_3B_3N_3Me_3$ is activated by η^6-coordination to a $Cr(CO)_3$ or $[Mn(CO)_3]^+$ fragment. Computational experiments replicated key experimental, structural, and spectroscopic metrics, which validated our computational parameters. With few exceptions, the calculated values matched our experimental ν_{CO} bands with an error of <20 cm^{-1} when the suggested correction factor (0.96)[50] was applied (Table S-1†). For instance, the calculated C=O stretching frequencies of 2069, 2002, and 2001 cm^{-1} agree well with the experimentally observed bands at 2072 and 1997 for compound **2**. Additionally, the calculated redox potentials (Table S-2†) are likewise in good agreement with experimental data (when available). For instance, the calculated potential of −1.49 V (*vs.* $Cp_2Fe^{0/+}$) for the single electron reduction of **2** in Et_2O agrees well with the experimental value of −1.38 V (*vs.* $Cp_2Fe^{0/+}$).

2.2. Effect of metal coordination on pK_a and ΔG_{H^-} of $Me_3B_3N_3Me_3$

The C–C bonds of arenes are typically reduced by non-polar reagents (*e.g.* metal dihydrides and H_2 with a variety of heterogeneous catalysts),[51,52] though some exceptions have been reported.[53–55] In contrast, the B=N bonds of borazine require polar reagents for reduction, and thus, the two properties of borazines most relevant to ionic hydrogenation, pK_a (Table S-4†) and hydricity (Scheme 3), were evaluated. Based on the absence of reactivity with hydride sources and many relatively strong acids,[27,56] the free borazines are predicted to be inert to hydride addition and protonation. In contrast, coordination to a metal fragment induces dramatic changes in both of these values. The conjugate acid strength of the borazine ligand was increased (became a stronger acid) by 13 and 44 pK_a units when coordinated in an η^6-fashion to $Cr(CO)_3$ and $[Mn(CO)_3]^+$ fragments, respectively. Furthermore, a dramatic decrease (>30 kcal mol^{-1}) in the thermodynamic hydricity (became a poorer hydride donor) was observed for the corresponding hydrides [($Me_3B_3N_3Me_3$)(μ-H)$Cr(CO)_3$]Li (**3**; ΔG_{H^-} = 41 kcal mol^{-1}) and ($Me_3B_3N_3Me_3$)(μ-H)$Mn(CO)_3$ (**4**; ΔG_{H^-} = 69 kcal mol^{-1}) when compared to [$Me_3B_3HN_3Me_3$]$^-$. This is in agreement with our previous experimental results which showed that $[Et_3BH]^-$ (ΔG_{H^-} = 23) was competent for hydride delivery to both metal complexes, but not to free $Me_3B_3N_3Me_3$.[27,28] A NICS(0) calculation showed substantial reductions in the aromatic character upon hydride addition. Furthermore, when the ratio of the NICS(0) values between **1**/**3** and **2**/**4** was compared, a greater change in the aromaticity of the hexamethylborazine ring was noted for the former pair (see ESI, Table S-6†). This result suggests that hydride addition to $Cr(CO)_3$ results in a greater decrease in the aromaticity than the corresponding $[Mn(CO)_3]^+$ unit.

Due to the high energy cost associated with hydride sources such as $[HBEt_3]^-$,[57] these reagents have limited application in B–N spent fuel regeneration schemes. In contrast, metal hydrides derived from H_2 have thermodynamic hydricity values that are tunable and can be of similar strength to many non-metal hydrides,[58–61] and thus are attractive candidates for the development of low-energy regeneration pathways. Using the computed hydricity values to guide selection of a suitable hydride candidate, we evaluated the hydride transfer to **1** using $HCo(dmpe)_2$, (ΔG_{H^-} = 37 kcal mol^{-1}, dmpe = 1,2-bis(dimethylphosphino)ethane), which is an H_2-derived hydride[61] and much milder than $LiEt_3BH$ (ΔG_{H^-} = 23.2 kcal mol^{-1}).[27] Consistent with the calculated thermodynamic hydricities, when **1** was allowed to react with 1 eq. of $HCo(dmpe)_2$ at −40 °C in 2-Me-THF, the hydride adduct (**3**) was obtained, as confirmed by NMR and IR spectroscopy. This finding is significant, as the delivery of H_2-derived reducing equivalents to B=N spent fuels has previously been a coveted goal for any regeneration cycle.[25,61]

2.3. Protonation reactions of dearomatized hydride adducts

Following hydride delivery, protonation reactions afford the partially saturated 1,2-H_2-adduct, which completes B=N bond reduction. Our previous experimental studies suggested that the products obtained from these reactions were highly dependent on the proton source, as well as the specific reaction conditions employed.[27,28] In all cases, the products formed from the addition of acid were too unstable to be isolated and fully characterized, and further reactions with excess HX were used

to trap the reactive intermediates by adding across the remaining B=N bond(s). The substituted cyclotriborazanes $(OAc^F)_2Me_4B_3N_3Me_3D_3$ and $(OAc^F)_3Me_3B_3N_3Me_3D_3$ (OAc^F = CF_3COO^-) were obtained following treatment of $[(Me_4B_3N_3Me_3)Cr(CO)_3]MgBr$ or $Me_3B_3N_3Me_3$ with excess trifluoroacetic acid ($HOAc^F$). The former results from the trapping of the putative intermediate $(Me_4B_3N_3Me_3H)Cr(CO)_3$ wherein a borazine B=N bond has been reduced by the sequential addition of a Me^- nucleophile and a proton.[27]

Given the challenges associated with studying such 1,2-H_2-intermediates due to their limited stability, the feasibility of these reactions was explored computationally. For these studies, we evaluated both the relative basicity of the nitrogen atoms at the 2 and 4-positions, as well as at the hydride ligand (Scheme 4). Additionally, the free energy of hydrogen elimination from the 1,2-H_2-adduct was calculated in order to assess its relative stability. Not surprisingly, H_2 elimination is predicted to be favored by >20 kcal mol^{-1} from both metal complexes. This is consistent with our experimental data which suggests that the partially saturated borazine species are highly unstable. However, the basicity of both the hydride and the 2-position nitrogen atom are predicted to be within 5 pK_a units for both complexes ($\Delta pK_a = 4.3$ for Mn and 4.1 for Cr). This is consistent with the experimental observations, *vide supra*, and suggests that such intermediates might be transiently accessible, and could be intercepted during a catalytic regeneration scheme.

2.4. Single electron transfer to 2 and subsequent reactivity

One of the main motivations for studying the coordination chemistry of borazines is to uncover low energy routes to generate new B–H bonds. The delivery of hydrides generated from electrons and hydrogen atoms (or protons) would be advantageous if reductions could be carried out at modest operating potentials. Complex **2** displays two reduction events at −1.19 and −1.70 V *vs.* $FeCp_2$ (0.05 M [^{n}Bu$_4$N][BAr′$_4$]; BAr′$_4$ = tetrakis-3,5-trifluoromethyl-phenyl borate) in 2-MeTHF, and at −1.38 and −1.88 V in 0.1 M ^{n}Bu$_4$NPF$_6$/CH_2Cl_2, the first of which is quasi-reversible in both solvent systems. Prior work demonstrated that 2 eq. of Na/$C_{10}H_8$ and 1 eq. of $HOAc^F$ can be used to generate a hydride complex, $(Me_3B_3N_3Me_3)(\mu\text{-}H)Mn(CO)_3$ (**4**), from **2**, through protonation of the reduced Mn center. As an alternative low-energy pathway, we targeted the 1 e^- reduction of **2** as a potential intermediate en route to the hydride, **4**.

To explore single electron reductions of **2**, we allowed **2** to react with a single equivalent of the mild reductant, Cp_2Co (−1.30 V *vs.* $Fc^{0/+}$).[62] The reduction proceeded readily when 1 eq. of Cp_2Co was added to a frozen 2-Me-THF solution of **2** (Fig. 1A). The resulting complex (**5**) was characterized by EPR spectroscopy (Fig. 1C), which revealed a rhombic spectrum ($g_x = 2.0238$, $g_y = 2.0269$, $g_z = 1.9803$) with hyperfine coupling interactions to ^{55}Mn ($A_{^{55}Mn}$ = 169.7, 184.8, 223.8 mHz) and ^{14}N ($A_{^{14}N}$ = 107.8, 62.2, 119.1 mHz) nuclei. Further confirmation of single electron reduction was afforded by an Evans method analysis of a solution of **5** which revealed a $\mu_{eff} = 1.92$, consistent with an s = 1/2 system. A solution IR spectrum of **5**, revealed new ν_{CO} bands at 2011, 1944, and 1930 cm^{-1}. The 61 cm^{-1} bathochromic shift of the A′ band is consistent with a C_s symmetric reduced $Mn(CO)_3$ fragment. The lowered symmetry is likely the result of ring slippage from η^6 to η^4 upon reduction.[63] Characterization of **5** by X-ray diffraction was precluded by its thermal instability.[64] However, calculations provided insight into product structure. Importantly, a $\Delta\nu_{CO}$ of 58 cm^{-1} was also predicted from theory, and the complex minimized to a structure featuring an η^6 to η^4 hapticity shift of the borazine unit. The calculated SOMO (Fig. 1B) is distributed between the $Mn(CO)_3$ fragment and the nitrogen p-orbitals, which is consistent with the observed ^{14}N hyperfine coupling.

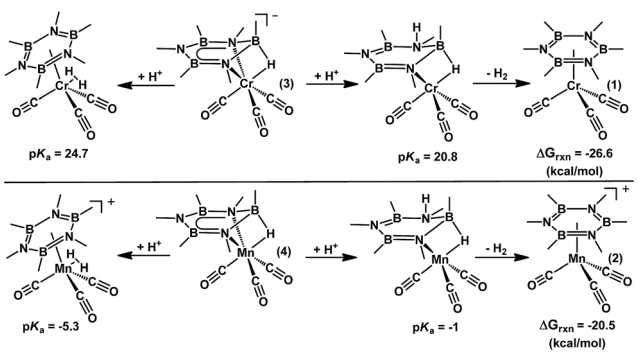

Scheme 4 Calculated pK_a values, and free energy of H_2 loss, for borazine hydride adducts **3** and **4** in Et_2O solution.

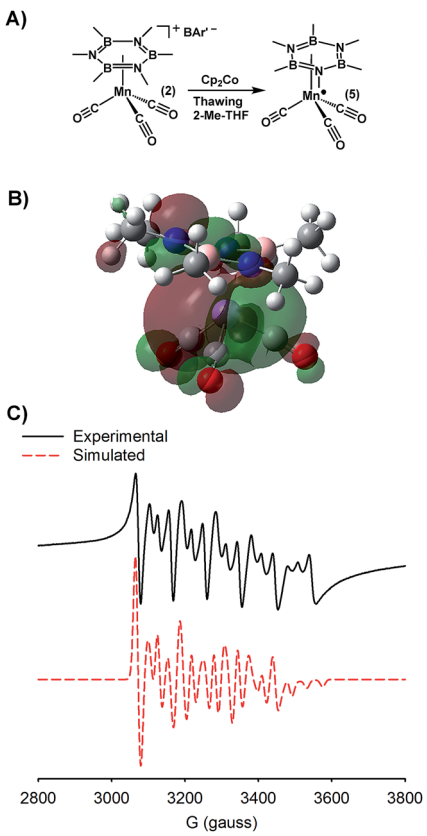

Fig. 1 (A) Synthetic scheme for generation of reduced complex **5**. (B) Calculated SOMO of **5**. (C) Experimental (black) and simulated (red) X-band EPR spectra of **5**.

2.5. Anthraquinone mediated reduction of 2 to 4

Following the single electron reduction to afford **5**, we assessed the viability of completing a hydrogen-atom transfer to the Mn–borazine unit. Quinones have been shown to act as redox mediators,[65,66] and to abstract H-atoms from sacrificial sources (including solvents) when reduced under conditions that promote single electron transfer.[67–69] These reactions afford reduced hydroquinone salts, that contain hydridic O–H bonds.[70]

Based on our evaluation of hydride donor requirements for **2**, we targeted a hydride reagent derived from a single equivalent of a reductant and an H-atom source. 9,10-anthraquinone (AQ) was selected because its corresponding hydroquinone salt (**6**) is sufficiently hydridic (37.2 kcal mol^{-1}) to react with **2** to form **4**. Consistent with our theoretical prediction of the hydricity of **4**, when a mixture of AQ and **2** (1 : 1) was treated with Cp_2Co (1 eq.) in thawing 2-Me-THF (Scheme 5), **4** was obtained in 90% yield. A control reaction showed no reaction occurred when combining Cp_2Co with AQ in the absence of **2**. This is consistent with the similar reduction potentials of Cp_2Co and AQ (−1.3 *vs.* −1.2 V, *vs.* $Fc^{0/+}$, respectively) in 2-Me-THF (0.05 M [$^nBu_4N$][BAr'_4]). We note that the redox potential for the reduction of quinones is highly sensitive to hydrogen bonds and Lewis acid/base interactions with the quinone C=O bond.[71–74] Coordinated borazine likely acts as a Lewis acid in this regard, and consistent with a persistent interaction in solution, the anthraquinone wave is anodically shifted by ~400 mV, (Fig. S12†) when **2** is also present in the solution. This redox tuning enables reduction of AQ to its corresponding semiquinone by Cp_2Co. Following reduction, generation of the anthrahydroquinone salt, **6**, likely results from H-atom transfer from the solvent to the semiquinone species, which can then transfer a hydride to **2**.

The anthrahydroquinone salt, **6**, was independently prepared from the reaction of $NaEt_3BH$ with AQ, in order to verify its competence as a hydride donor to **2**. Upon introduction of **6** to **2**, complex **4** was afforded in 65% yield. No activity for reduction and/or hydride transfer was noted when **6** was replaced with *p*-benzoquinone, whose hydroquinone salt is a much weaker hydride donor ($\Delta G_{H^-} = 56.7$ kcal mol^{-1}).[75] Furthermore, attempts to reduce **2** with *p*-benzoquinone and Cp_2Co yielded none of the desired product under identical conditions. These results suggest that mixtures of **6** and **2** are thermodynamically matched to promote reduction and hydride addition.

2.6. Proposed mechanism of anthraquinone mediated hydride transfer

The anthrahydroquinone salt (**6**) that delivers a hydride to **2**, *vide supra*, can be generated from the parent anthraquinone by either H-atom transfer (from solvent) or protonation pathways.[66,67,70] To differentiate between these two limiting pathways, we evaluated whether an exogenous H-atom donor, such as solvent, participated in an H-atom transfer pathway to generate **6**.[66,67,70] The substitution of the 2-Me-THF solvent with C_6F_6, a solvent without hydrogen atoms, provided **4** in only trace amounts (<10%).[76] Furthermore, the addition of 2 eq. of H_2O to the reaction carried out in C_6F_6 also did not afford **4**, which is inconsistent with adventitious water acting as the hydrogen donor. The reduction also proceeds readily (65% yield) when dichloromethane (CH_2Cl_2), a solvent with similar C–H BDFE values (86.4 kcal mol^{-1} *vs.* 81.7 kcal mol^{-1} for 2-Me-THF), is substituted as the reaction solvent, suggesting that solvents with comparable BDFE values can be used as H-atom donors to drive the reaction.

Calculation of the homolytic bond dissociation free energies (BDFE) for both **6** and **4**, afforded values of 39.0 and 52.8 kcal mol^{-1} respectively, which are significantly lower than that of 2-Me-THF (81.7 kcal mol^{-1}, Table S-4†). However, when the THF coupling product is included, the net reaction to reduce anthrasemiquinone to **6** is decreased to 12.5 kcal mol^{-1} (Scheme S-1†). Moreover, the reduction of **2** to **4**, when using **6** as the hydride source, is exergonic by 31.5 kcal mol^{-1}. The difference between these two reaction energies results in an overall free energy of −19 kcal mol^{-1} (Scheme 6). Furthermore, when identical calculations were carried out using CH_2Cl_2 as the H-atom donor (assuming formation of 1,1,2,2-tetrachloroethane as the radical coupling byproduct) the net reaction energy is −7.4 kcal mol^{-1}. Thus, the products are sufficiently stable to drive the reaction forward and promote cleavage of the relatively strong solvent C–H bonds.

2.7. AQ mediated hydride reduction of 2 by applied potential

Electrochemical experiments were explored to further evaluate whether single or two electron redox pathways are operative to generate boron hydrides. The number of electron equivalents can be explicitly regulated during a controlled potential electrolysis, and thus can easily differentiate between single/two electron pathways. Furthermore, the operating potential can

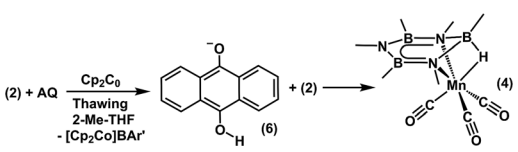

Scheme 5 Proposed mechanism of AQ mediated hydride reduction of **2** to **4**.

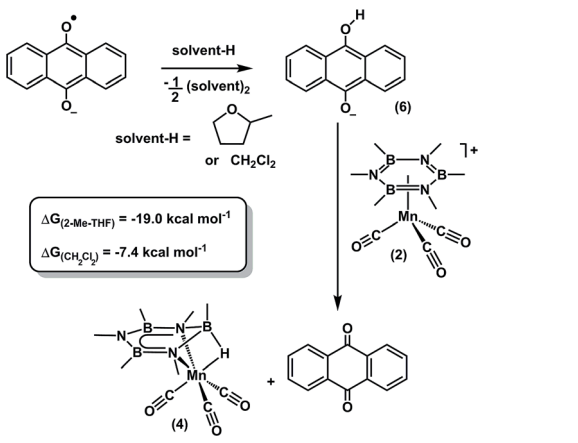

Scheme 6 Proposed net reaction, and calculated free energy, for formation of **2** *via* AQ mediated H-atom transfer in 2-MeTHF and CH_2Cl_2.

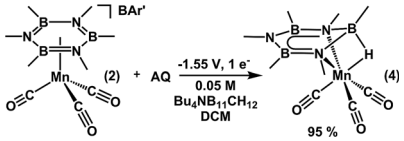

Scheme 7 Conversion of **2** to **4** by bulk electrolysis.

also be selected to coincide with a given redox event observed in the cyclic voltammogram.

The selection of an appropriate solvent/electrolyte combination required careful consideration. For instance, when using $[^nBu_4N]PF_6$ as the supporting electrolyte, fluorine transfer from the electrolyte was a competing side-reaction (40% yield) under the coulometry experimental conditions.[77] Competitive fluorine transfer to borazine is perhaps not surprising, given the extremely high B–F bond strength (183 kcal mol^{-1}).[78] In an effort to circumvent F-transfer to the borazine, we targeted a fluorine-free solvent-electrolyte system for bulk electrolysis. Unfortunately, the high lability of the borazine unit further complicated solvent/electrolyte selection. For instance, borazine was displaced from the metal center with common electrolytes such as $[^nBu_4N]ClO_4$ and $[^nBu_4N]Cl$, as well as in solvents such as tetrahydrofuran and acetonitrile. As an alternative, we turned to the $[^nBu_4N]^+$ salt of mono-carborane ($CB_{11}H_{12}^-$), as carborane electrolytes have been shown to be weakly coordinating anions that have high solubility and possess high electrochemical stability.[79,80]

Controlled potential electrolysis was conducted in a 0.05 M CH_2Cl_2 solution of $[^nBu_4N][CB_{11}H_{12}]$ at −1.55 V (*vs.* $Fc^{0/+}$). Gratifyingly, after the passage of 4.07 coulombs (0.049 mmol) to a 0.049 mmol solution of **2**, **4** was obtained in 95% yield (Scheme 7) based on integration of the ^{11}B NMR spectrum using $(TMSO)_3B$ as an internal standard (Fig. S6†). For further confirmation, the solution-cell IR spectrum was collected and **4** was the primary carbonyl containing species observed. Of particular note, the reaction yield of 95% after passing 1 eq. e^- implies an operative single electron process, compared to a 2 e^- process, where less than 50% yield would be expected. In agreement with our chemical reduction reactions, **4** was not observed when bulk electrolysis was conducted in the absence of 9,10-anthraquinone. Collectively, these results provide strong evidence that reduction of the borazine unit occurs through a single electron H-atom transfer pathway that is mediated by anthraquinone. The energy input required for this transformation is significantly lower than that required for a $2e^-/H^+$ reduction sequence.

3. Conclusions

Through a combination of computational and experimental studies, this study has established a low-energy pathway to reduce borazines, which are models for spent B–N fuels. Coordination of borazine to a $M(CO)_3$ unit was found to dramatically change the requirements for hydride and proton transfer to the borazine unit. A decrease (>30 kcal mol^{-1}) in the thermodynamic hydricity (complexes became more likely to accept a hydride) between free and coordinated borazines was imparted by coordination to $Cr(CO)_3$ and $[Mn(CO)_3]^+$ fragments. This change in the hydride accepting ability accounted for the distinct hydride addition reactivity observed for free *vs.* metalated borazines. Hydricity values were also demonstrated to vary significantly with metal oxidation state. Importantly, borazine dearomatization *via* hydride addition was verified as the key first step in such a reduction scheme. Calculated hydricity requirements for borazine dearomatization were used to demonstrate hydride delivery from an H_2-derived hydride source, and importantly, to uncover a unique hydride delivery mechanism which proceeds through a single electron reduction and H-atom transfer reaction, mediated by anthraquinone. The latter transformation was also carried out electrochemically, at relatively positive potentials by comparison to all prior reports, thus establishing an important proof of concept for any future electrochemical B=N bond reduction sequences. These efforts may find utility in future regeneration schemes for spent AB fuels as well as other B–N heterocycles that are promising H_2 storage molecules.

4. Experimental section

4.1. Computational details

All structures were fully optimized without symmetry constraints using either the M06-2X[81] or the B3LYP[82–85] functional as implemented in Gaussian 09,[86] using the 6-31G** basis set.[87,88] The ultrafine integration grid was employed in all calculations, which ensured the stability of the optimization procedure for the investigated molecules. Each stationary point was confirmed by a frequency calculation at the same level of theory to be a real local minimum on the potential energy surface without imaginary frequency. More accurate electronic energies were computed for the optimized geometries using the larger 6-311++G(d,p) basis set.[89,90] All reported free energies are for Et_2O solution at the standard state ($T = 298$ K, $P = 1$ atm, 1 mol L^{-1} concentration of all species in Et_2O) as modelled by the polarized continuum model.[91] The energy values given in the paper correspond to solvent-corrected Gibbs free energies that are based on B3LYP/6-311++G(d,p) electronic energies and all corrections calculated at the B3LYP/6-31G(d) level. All calculated pK_a values are for Et_2O solutions. Although no pK_a scales have been experimentally determined in diethyl ether, we chose to employ $[Et_3NH]^+$ as the anchor of our pK_a scale and assign it a pK_a value of 12.5. A value of 12.5 was chosen because $[Et_3NH]^+$ has been previously employed as an anchor (pK_a value of 12.5) for a structurally similar solvent, THF.[35,36] Initial optimizations employed the M06-2X functional as the included dispersion corrections have been shown to provide better estimation of main-group systems.[37,81,92] Although computations employing the M06-2X functional better modeled the thermochemistry of borazine and hexamethylborazine, all computations reported within made use of the B3LYP functional, which was found to model the manganese and chromium complexes better than the M06-2X functional. All computational vibrational frequencies reported within employed a scaling factor of 0.96.[50]

4.2. General experimental procedures

All experiments were conducted using standard Schlenk techniques or in a nitrogen filled glovebox. NMR spectra were recorded on Varian MR400, vnmrs 500, or vnmrs 700 MHz spectrometers. ^{1}H spectra were referenced relative to the residual solvent resonance, and ^{11}B, and ^{19}F spectra were referenced indirectly based on the ^{1}H spectrum.[93] IR spectra were recorded on a Nicolet iS-10 spectrometer from Thermo Scientific in a KBr plate solution cell. X-band EPR spectra were recorded on a Bruker EMX ESR spectrometer equipped with a 4102-ST cavity. EPR simulations were conducted using the EasySpin software package for MATLAB.[94] Mass spectra were collected by electron impact ionization on a VG 70-250-S magnetic sector, double-focusing mass spectrometer. The electron energy was set to 70 eV, and the source temperature was 240 °C. Nominal mass spectra were obtained scanning the magnet from *m*/*z* 1000 to *m*/*z* 35 at 8 seconds per decade, using an external mass calibration. Evan's method was conducted using a coaxial NMR tube insert from Wilmad glass with benzene or dichloromethane added to samples as the diamagnetic reference compound. 9,10-anthraquinone and *p*-benzoquinone were obtained from Sigma Aldrich and recrystallized from ethyl-acetate before use. Cobaltocene (Cp_2Co) was purchased from Strem chemicals and used as received. $HCo(dmpe)_2$ was prepared by a previously reported procedure.[61] $[^{n}Bu_4N][CB_{11}H_{12}]$ was prepared by reacting the commercially available $Cs[CB_{11}H_{12}]$ with $[^{n}Bu_4N]Cl$ in aqueous solution. The resulting precipitate was isolated by filtration and dried under vacuum at 100 °C for 48 h. $(Me_3B_3N_3Me_3)Cr(CO)_3$ and $[(Me_3B_3N_3Me_3)Mn(CO)_3][BAr'_4]$ were synthesized by previously reported routes.[27,28] All solvents were passed through an S.G. Waters solvent purification system or dried and degassed by standard methods.[95] All other chemicals were purchased from commercial vendors and used as received. All filtrations were conducted using a pipet blocked with Whatman glass fiber filter paper.

Reaction of 1 with $HCo(dmpe)_2$. A solution of **1** (9.1 mg, 0.03 mmol) was prepared in 1 ml 2-Me-THF. The solution was frozen, and $HCo(dmpe)_2$ (9.1 mg, 0.03 mmol) was added. The mixture was thawed and shaken vigorously for 20 seconds, and then transferred to an NMR tube. The ^{11}B NMR spectrum (Fig. S-1†) was consistent with formation of **4** in 30% yield.

Preparation of $Mn(\mu\text{-}H)(Me_3B_3N_3Me_3)(CO)_3$ (4) by reduction with Cp_2Co and AQ. A solution containing **2** (16.7 mg 0.014 mmol) and 9,10-anthraquinone (3.0 mg, 0.014 mmol) in 1 ml 2-Me-THF was frozen in the glovebox cold-well inside a 20 ml scintillation vial. To the frozen solution was added solid Cp_2Co (2.7 mg 0.014 mmol). The mixture was then allowed to thaw and the capped vial vigorously shaken for 30 seconds. The solution was then thawed to room temperature and the yield (85%) of the hydride **4** was determined by ^{11}B NMR (Fig. S-2†) integration using the residual $BAr'_4{}^{-}$ salt as an internal standard.[28] As previously noted, the spectroscopic properties of **4** are highly sensitive to the solution environment.[28] Slight differences in the ^{11}B NMR are observed from that previously reported (Fig. S-3†), because of this, solution cell IR was also used to confirm the identity of the product (Fig. S-7†).

Preparation of $Mn(\mu\text{-}H)(Me_3B_3N_3Me_3)(CO)_3$ (4) by bulk electrolysis. A solution of **2** (57.2 mg, 0.049 mmol) and 9,10-anthraquinone (10.2 mg, 0.049 mmol) in 7 ml $[^{n}Bu_4N]B_{11}CH_{12}$ electrolyte solution (0.05 M in CH_2Cl_2) was prepared and placed in the working electrode chamber of a bulk electrolysis cell. The counter electrode chamber was filled with an electrolyte solution and equipped with a nickel gauze electrode. Cyclic voltammetry was recorded in the working electrode chamber (GC working electrode, Ag/AgCl reference electrode) and the potential for bulk electrolysis (−1.55 V *vs.* $Fc^{0/+}$) was selected to be coincident with first observed redox couple for anthraquinone. The cell was then equipped with a carbon felt working electrode and bulk electrolysis was conducted until a total charge of 4.07C (1 e^{-} relative to Mn) was passed. Electrolysis was then stopped, and the solution from the working electrode chamber was removed, and reduced to a total volume of 1 ml under vacuum. This solution was then characterized by ^{11}B NMR, and total yield of the hydride was determined based on the relative ^{1}H NMR integration against a $B(OTMS)_3$ (18 ppm in ^{11}B NMR) internal standard (16.6 μl, 0.049 mmol) added after electrolysis.

Preparation of $Mn(Me_3B_3N_3Me_3)(CO)_3$ (5). A solution of **1** (20.0 mg, 0.017 mmol) in 0.75 ml 2-Me-THF was prepared and the solution was frozen in the glovebox coldwell inside a 20 ml scintillation vial. To the frozen solution, solid Cp_2Co (3.6 mg, 0.017 mmol) was added. The mixture was then allowed to thaw for 30 seconds with vigorous shaking. The red/orange solution was then refrozen to obtain a mixture containing $[Cp_2Co][BAr'_4]$ and the reduced Mn complex **5** that was characterized without further workup. **5** proved to be highly thermally sensitive, thus, solutions of **5** were stored either frozen or at −78 °C to prevent thermal decomposition. IR (2-Me-THF): ν_{CO} 2011, 1944, 1930 cm^{-1}; X-Band EPR (77 K) $g_x = 2.0238$ $g_y = 2.0269$ $g_z = 1.9803$ (Gauss), hyperfine coupling: ^{14}N (107.8, 62.2, 119.1) ^{55}Mn (169.7, 184.8, 223.8) (mHz); Evan's method (2-Me-THF): diamagnetic additive: C_6H_6, peak separation = 0.20 ppm, $\mu_{eff} = 1.92$, $N = 1.17$.

Acknowledgements

The authors are grateful to Dr Michael Mock for a generous donation of the $HCo(dmpe)_2$ used in this manuscript. This work was supported by the University of Michigan Department of Chemistry (NKS) and by startup funds from Washington State University (ZMH). NKS is an Alfred P. Sloan Research Fellow.

Notes and references

1 N. S. Lewis and D. G. Nocera, *Proc. Natl. Acad. Sci. U. S. A.*, 2006, **103**, 15729–15735.
2 M. Z. Jacobson, *Energy Environ. Sci.*, 2009, **2**, 148–173.
3 J. Graetz, *Chem. Soc. Rev.*, 2009, **38**, 73–82.
4 Q.-L. Zhu and Q. Xu, *Energy Environ. Sci.*, 2015, **8**, 478–512.
5 http://www1.eere.energy.gov/vehiclesandfuels/pdfs/program/hstt_roadmap_june2013.pdf.
6 Z. Huang and T. Autrey, *Energy Environ. Sci.*, 2012, **5**, 9257–9268.

7 W. Luo, P. G. Campbell, L. N. Zakharov and S.-Y. Liu, *J. Am. Chem. Soc.*, 2011, **133**, 19326–19329.
8 N. C. Smythe and J. C. Gordon, *Eur. J. Inorg. Chem.*, 2010, **2010**, 509–521.
9 A. Staubitz, A. P. M. Robertson and I. Manners, *Chem. Rev.*, 2010, **110**, 4079–4124.
10 F. H. Stephens, V. Pons and R. Tom Baker, *Dalton Trans.*, 2007, 2613–2626.
11 R. J. Keaton, J. M. Blacquiere and R. T. Baker, *J. Am. Chem. Soc.*, 2007, **129**, 1844–1845.
12 T. Wideman, P. J. Fazen, A. T. Lynch, K. Su, E. E. Remsen, L. G. Sneddon, T. Chen and R. T. Paine, in *Inorganic Syntheses*, John Wiley & Sons, Inc., 2007, pp. 232–242, DOI: 10.1002/9780470132630.ch39.
13 J.-M. Yan, X.-B. Zhang, S. Han, H. Shioyama and Q. Xu, *Angew. Chem., Int. Ed.*, 2008, **47**, 2287–2289.
14 E. K. Mellon and J. J. Lagowski, *Advances in inorganic chemistry and radiochemistry*, Academic Press., New York, 1959.
15 E. L. Muetterties, *Boron hydride chemistry*, Academic Press, New York, 1975.
16 R. Boese, A. H. Maulitz and P. Stellberg, *Chem. Ber.*, 1994, **127**, 1887–1889.
17 R. Islas, E. Chamorro, J. Robles, T. Heine, J. Santos and G. Merino, *Struct. Chem.*, 2007, **18**, 833–839.
18 A. S. Lisovenko and A. Y. Timoshkin, *Inorg. Chem.*, 2010, **49**, 10357–10369.
19 M. H. Matus, K. D. Anderson, D. M. Camaioni, S. T. Autrey and D. A. Dixon, *J. Phys. Chem. A*, 2007, **111**, 4411–4421.
20 C. R. Miranda and G. Ceder, *J. Chem. Phys.*, 2007, **126**, 184703.
21 P. V. Ramachandran and P. D. Gagare, *Inorg. Chem.*, 2007, **46**, 7810–7817.
22 B. L. Davis, D. A. Dixon, E. B. Garner, J. C. Gordon, M. H. Matus, B. Scott and F. H. Stephens, *Angew. Chem., Int. Ed.*, 2009, **48**, 6812–6816.
23 A. D. Sutton, A. K. Burrell, D. A. Dixon, E. B. Garner, J. C. Gordon, T. Nakagawa, K. C. Ott, J. P. Robinson and M. Vasiliu, *Science*, 2011, **331**, 1426–1429.
24 C. Reller and F. O. R. L. Mertens, *Angew. Chem., Int. Ed.*, 2012, **51**, 11731–11735.
25 O. T. Summerscales and J. C. Gordon, *Dalton Trans.*, 2013, **42**, 10075–10084.
26 E. M. Leitao and I. Manners, *Eur. J. Inorg. Chem.*, 2015, **13**, 2199–2205.
27 T. J. Carter, J. W. Kampf and N. K. Szymczak, *Angew. Chem., Int. Ed.*, 2012, **51**, 13168–13172.
28 T. J. Carter, J. Y. Wang and N. K. Szymczak, *Organometallics*, 2014, **33**, 1540–1543.
29 P. G. Campbell, L. N. Zakharov, D. J. Grant, D. A. Dixon and S. Y. Liu, *J. Am. Chem. Soc.*, 2010, **132**, 3289–3291.
30 Y. Tan and X. Yu, *RSC Adv.*, 2013, **3**, 23879–23894.
31 W. R. Nutt and M. L. McKee, *Inorg. Chem.*, 2007, **46**, 7633–7645.
32 S. Bhunya, P. M. Zimmerman and A. Paul, *ACS Catal.*, 2015, **5**, 3478–3493.
33 H. S. Kang, *J. Phys. Chem. A*, 2005, **109**, 1458–1467.
34 A. J. Bridgeman, *Polyhedron*, 1998, **17**, 2279–2288.
35 K. Abdur-Rashid, T. P. Fong, B. Greaves, D. G. Gusev, J. G. Hinman, S. E. Landau, A. J. Lough and R. H. Morris, *J. Am. Chem. Soc.*, 2000, **122**, 9155–9171.
36 T. Rodima, I. Kaljurand, A. Pihl, V. Maemets, I. Leito and I. Koppel, *J. Org. Chem.*, 2002, **67**, 1873–1881.
37 L. Goerigk and S. Grimme, *Phys. Chem. Chem. Phys.*, 2011, **13**, 6670–6688.
38 R. Schellenberg, J. Kriehme and G. Wolf, *Thermochim. Acta*, 2007, **457**, 103–108.
39 Z. Chen, C. S. Wannere, C. Corminboeuf, R. Puchta and P. V. R. Schleyer, *Chem. Rev.*, 2005, **105**, 3842–3888.
40 P. V. R. Schleyer, B. Kiran, D. V. Simion and T. S. Sorensen, *J. Am. Chem. Soc.*, 2000, **122**, 510–513.
41 C. Corminboeuf, T. Heine and J. Weber, *Phys. Chem. Chem. Phys.*, 2003, **5**, 246–251.
42 A. Velian and C. C. Cummins, *Science*, 2015, **348**, 1001–1004.
43 N. D. Charistos, A. G. Papadopoulos and M. P. Sigalas, *J. Phys. Chem. A*, 2014, **118**, 1113–1122.
44 Werner and co-workers have characterized a $Cr(CO)_3$ complex of $H_3B_3N_3Me_3$ through ring metathesis, however, no structural data or reactivity studies for this complex have been reported.
45 K. Deckelmann and H. Werner, *Helv. Chim. Acta*, 1970, **53**, 139–141.
46 K. Deckelmann and H. Werner, *Helv. Chim. Acta*, 1971, **54**, 2189–2193.
47 J. J. Lagowski, *Coord. Chem. Rev.*, 1977, **22**, 185–194.
48 R. Prinz and H. Werner, *Angew. Chem., Int. Ed.*, 1967, **6**, 91–92.
49 H. Werner, R. Prinz and E. Deckelmann, *Chem. Ber.*, 1969, **102**, 95–103.
50 M. P. Andersson and P. Uvdal, *J. Phys. Chem. A*, 2005, **109**, 2937–2941.
51 P. J. Dyson, *Dalton Trans.*, 2003, 2964–2974.
52 L. Foppa and J. Dupont, *Chem. Soc. Rev.*, 2015, **44**, 1886–1897.
53 M. P. Boone and D. W. Stephan, *J. Am. Chem. Soc.*, 2013, **135**, 8508–8511.
54 M. P. Boone and D. W. Stephan, *Chem.– Eur. J.*, 2014, **20**, 3240.
55 T. Mahdi, Z. M. Heiden, S. Grimme and D. W. Stephan, *J. Am. Chem. Soc.*, 2012, **134**, 4088–4091.
56 Strong acids with nucleophillic anions (*e.g.* HCl) react readily with borazines through concerted addition. In our hands, Brookhart's acid ($HBAr'_4$) and $HCl:AlCl_3$ did not produce a reaction with borazine suggesting that protonated ether (pK_a = -9.7) is not sufficiently acidic to protonate borazine. To our knowledge, the only example of non-concerted borazine protonation was reported by Noth and co-workers, who used the superacid $HBr:AlBr_3$ in non-polar solvent. See: B. Gemünd, B. Günther and H. Nöth, *ARKIVOC*, 2008, 136.
57 *Ullmann's Fine Chemicals*, ed. B. Elvers, Wiley-VCH Verlag GmbH & Co. KGaA, Weinheim, Germany, 2014, vol. 3.
58 Z. M. Heiden and A. P. Lathem, *Organometallics*, 2015, **34**, 1818–1827.

59 C. J. Curtis, A. Miedaner, W. W. Ellis and D. L. DuBois, *J. Am. Chem. Soc.*, 2002, **124**, 1918–1925.
60 A. J. Price, R. Ciancanelli, B. C. Noll, C. J. Curtis, D. L. DuBois and M. R. DuBois, *Organometallics*, 2002, **21**, 4833–4839.
61 M. T. Mock, R. G. Potter, M. J. O'Hagan, D. M. Camaioni, W. G. Dougherty, W. S. Kassel and D. L. DuBois, *Inorg. Chem.*, 2011, **50**, 11914–11928.
62 N. G. Connelly and W. E. Geiger, *Chem. Rev.*, 1996, **96**, 877–910.
63 Attempts to verify the geometry of this species by paramagnetic ^{1}H NMR were unsuccessful as no signals were observed for complex **5**.
64 Slow decomposition was noted even when solutions of **5** were held at −78 °C.
65 X. Guo, H. Zipse and H. Mayr, *J. Am. Chem. Soc.*, 2014, **136**, 13863–13873.
66 N. Song, C. J. Gagliardi, R. A. Binstead, M.-T. Zhang, H. Thorp and T. J. Meyer, *J. Am. Chem. Soc.*, 2012, **134**, 18538–18541.
67 X. Ci, R. Silveira da Silva, D. Nicodem and D. G. Whitten, *J. Am. Chem. Soc.*, 1989, **111**, 1337–1343.
68 C. Rüchardt, M. Gerst and J. Ebenhoch, *Angew. Chem., Int. Ed.*, 1997, **36**, 1406–1430.
69 F. Wurche, W. Sicking, R. Sustmann, F.-G. Klärner and C. Rüchardt, *Chem.– Eur. J.*, 2004, **10**, 2707–2721.
70 X.-Q. Zhu and C.-H. Wang, *J. Org. Chem.*, 2010, **75**, 5037–5047.
71 J. Yuasa, T. Suenobu and S. Fukuzumi, *Chem. Phys. Chem.*, 2006, **7**, 942–954.
72 G. T. Cheek, *ECS Trans.*, 2013, **50**, 79–85.
73 J. Q. Chambers, in *The Quinonoid Compounds (1988)*, John Wiley & Sons, Inc., 2010, pp. 719–757, DOI: 10.1002/9780470772119.ch12.
74 R. S. Kim and T. D. Chung, *Bull. Korean Chem. Soc.*, 2014, **35**, 3143–3155.
75 We computationally investigated the possibility of dative bonding between AQ and **4**. The resulting complex of **4** and AQ is predicted to have a hydide donor abilitiy of 37 kcal mol^{-1}. See ESI† for additional details.
76 The C–H bonds of borazine are also possible H-atom donors, which can account for the 10% yield observed in C_6F_6.
77 See ESI† for additional details.
78 J. A. Dean and N. A. Lange, *Lange's handbook of chemistry*, McGraw-Hill, 1992.
79 T. J. Carter, R. Mohtadi, T. S. Arthur, F. Mizuno, R. Zhang, S. Shirai and J. W. Kampf, *Angew. Chem., Int. Ed.*, 2014, **53**, 3173–3177.
80 J. W. Johnson and A. H. Thompson, *J. Electrochem. Soc.*, 1981, **128**, 932–933.
81 Y. Zhao and D. G. Truhlar, *J. Chem. Theory Comput.*, 2008, **4**, 1849–1868.
82 A. D. Becke, *J. Chem. Phys.*, 1993, **98**, 5648–5652.
83 C. Lee, W. Yang and R. G. Parr, *Phys. Rev. B: Condens. Matter Mater. Phys.*, 1988, **37**, 785–789.
84 S. H. Vosko, L. Wilk and M. Nusair, *Can. J. Phys.*, 1980, **58**, 1200–1211.
85 P. J. Stephens, F. J. Devlin, C. F. Chabalowski and M. J. Frisch, *J. Phys. Chem.*, 1994, **98**, 11623–11627.
86 M. J. Frisch, G. W. Trucks, H. B. Schlegel, G. E. Scuseria, M. A. Robb, J. R. Cheeseman, G. Scalmani, V. Barone, B. Mennucci, G. A. Petersson, H. Nakatsuji, M. Caricato, X. Li, H. P. Hratchian, A. F. Izmaylov, J. Bloino, G. Zheng, J. L. Sonnenberg, M. Hada, M. Ehara, K. Toyota, R. Fukuda, J. Hasegawa, M. Ishida, T. Nakajima, Y. Honda, O. Kitao, H. Nakai, T. Vreven, J. A. Montgomery Jr., J. E. Peralta, F. Ogliaro, M. Bearpark, J. J. Heyd, E. Brothers, K. N. Kudin, V. N. Staroverov, T. Keith, R. Kobayashi, J. Normand, K. Raghavachari, A. Rendell, J. C. Burant, S. S. Iyengar, J. Tomasi, M. Cossi, N. Rega, J. M. Millam, M. Klene, J. E. Knox, J. B. Cross, V. Bakken, C. Adamo, J. Jaramillo, R. Gomperts, R. E. Stratmann, O. Yazyev, A. J. Austin, R. Cammi, C. Pomelli, J. W. Ochterski, R. L. Martin, K. Morokuma, V. G. Zakrzewski, G. A. Voth, P. Salvador, J. J. Dannenberg, S. Dapprich, A. D. Daniels, O. Farkas, J. B. Foresman, J. V. Ortiz, J. Cioslowski and D. J. Fox, *Gaussian 09, Revision D.01*, Gaussian, Inc., Wallingford, CT, 2013.
87 J. D. Dill and J. A. Pople, *J. Chem. Phys.*, 1975, **62**, 2921–2923.
88 W. J. Hehre, R. Ditchfield and J. A. Pople, *J. Chem. Phys.*, 1972, **56**, 2257–2261.
89 R. Krishnan, J. S. Binkley, R. Seeger and J. A. Pople, *J. Chem. Phys.*, 1980, **72**, 650–654.
90 M. M. Francl, W. J. Pietro, W. J. Hehre, J. S. Binkley, M. S. Gordon, D. J. DeFrees and J. A. Pople, *J. Chem. Phys.*, 1982, **77**, 3654–3665.
91 M. Cossi, N. Rega, G. Scalmani and V. Barone, *J. Comput. Chem.*, 2003, **24**, 669–681.
92 Y. Zhao and D. G. Truhlar, *Theor. Chem. Acc.*, 2008, **120**, 215–241.
93 R. K. Harris, E. D. Becker, S. M. C. D. Menezes, R. Goodfellow and P. Granger, *Pure Appl. Chem.*, 2001, **73**, 1795–1818.
94 S. Stoll and A. Schweiger, *J. Magn. Reson.*, 2006, **178**, 42.
95 W. L. F. Armarego and C. L. L. Chai, *Knovel and ScienceDirect, Purification of Laboratory Chemicals*, Elsevier/Butterworth-Heinemann, Amsterdam, Boston, 2009.